



ORIGINAL ARTICLE

Adopting a green method for the synthesis of gold nanoparticles on cotton cloth for antimicrobial and environmental applications



Yasir Anwar^a, Ihsan Ullah^a, Mazhar Ul-Islam^b, Khalid M Alghamdi^a, Ashi Khalil^c, Tahseen Kamal^d

^a Department of Biological Sciences, Faculty of Science, King Abdulaziz University, Jeddah, Saudi Arabia

^b Department of Chemical Engineering, College of Engineering, Dhofar University, Salalah, Oman

^c Institute of Chemical Sciences, University of Peshawar, Pakistan

^d Center of Excellence for Advanced Materials Research, King Abdulaziz University, P. O. Box 80203, Jeddah 21589, Saudi Arabia

Received 1 May 2021; accepted 6 July 2021

Available online 16 July 2021

KEYWORDS

Coating;
Au nanoparticles;
Nitrophenol;
Antimicrobial;
Cotton cloth

Abstract In this research, a simple and green approach towards preparation of biogenic gold nanoparticles on cotton cloth (AuNPs-CC) was developed. It was found that the hydroxyl functional groups of the cellulose macromolecules, abundantly available in cotton, slowly reduced the Au ions to nanoparticles. To help accelerate the kinetic process of AuNPs formation, a *Citrus limon* juice concentrate was utilized. The samples were characterized by field emission scanning electron microscope (FESEM), energy-dispersive spectroscopy (EDS) and other spectroscopic methods. The FESEM images directly showed the ~22 nm size AuNPs attached to the cotton cloth fibers. The XPS and XRD confirmed the formation of biogenic AuNP over CC surface. The pristine-CC and AuNPs-CC were studied for their antibacterial properties using their different strains. Moreover, AuNPs-CC was used as a catalyst in the pollutants degradation (*para*- and *ortho*-nitrophenol) in their aqueous solutions. The AuNP-CC catalyzed the *p*-NP and *o*-NP reductions with high reaction rate constants. Moreover, the *Citrus limon* assisted synthesized AuNP-CC has antibacterial activities for pathogenic bacteria.

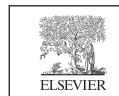
© 2021 The Author(s). Published by Elsevier B.V. on behalf of King Saud University. This is an open access article under the CC BY-NC-ND license (<http://creativecommons.org/licenses/by-nc-nd/4.0/>).

1. Introduction

Porosity and good hydrophilic properties of the cotton cloth are just suitable growing environments for different microorganisms (Ali et al., 2017b; Cerkez et al., 2012). Upon finding suitable conditions for growth, pathogenic bacteria can proliferate on the cotton cloth and develop and grow in the form of colonies. This leads to the production of unpleasant smell,

E-mail address: yanwarulhaq@kau.edu.sa (Y. Anwar)

Peer review under responsibility of King Saud University.



Production and hosting by Elsevier

spots, demising and fading of the fabric color. Of these, the cotton cloths used in hospitals are highly prone to pathogenic microorganisms (Ganesan and Gurumallesh Prabu, 2019). Their growth plays a vehicle role in spreading of infectious diseases among the patients and interacting humans. To overcome or limit the above described issues, huge efforts have been made to produce the antimicrobial cotton fabrics (Cerkez et al., 2012; Ganesan and Gurumallesh Prabu, 2019). This has been achieved by using antimicrobial coating agents adhered to the cotton textiles, such as quaternary ammonium compounds, poly(hexamethylene biguanide), N-halamine, benzophenones, chitosan, metals and metal salts as well as metallic oxides (Cerkez et al., 2012; Hou et al., 2015; Ng et al., 2020). Today it is well known that some microorganisms are infamously resistant to disinfectants and other developed antibiotics (Subirats et al., 2020). The existence of such microorganisms in our surroundings are a serious threat to the human health (Martin et al., 2020). For that reason, it is of high concern to obtain antimicrobial surfaces which inhibit the antibiotic resistant bacteria (Xiao et al., 2020, p.).

Presence of toxic dyes and other hazardous compounds such as nitroarenes in our environment are serious issues which should be resolved to save the humans, animals and plants lives (Ahmed et al., 2016a; Ali et al., 2019; Anwar, 2018; Anwar and Alghamdi, 2020). These toxic chemicals mostly come from different industries to the outer environment through water channels (Ali et al., 2018b; Ali et al., 2020a). Therefore, the degradation of the mentioned compounds is of great industrial and environmental importance (Ali et al., 2020b; Ceylan and Aydin, 2020). Recently, the development of photo-catalytically degradation of the toxic compounds have revolutionized the world. However, photo-catalytic degradation is a slow process (Ali et al., 2020c) and therefore, an alternate reduction process of the coloring compounds to colorless non-harmful compounds are attractive studies these days (Kamal et al., 2016a, 2017a; Khan et al., 2017). A famous example of one of the pollutants is the 4-nitrophenol (Kamal et al., 2016a). This compound is known to cause a serious damage to the central nervous systems, and other organs of the animals found in water bodies and humans. The compound is known to be highly stable and even strong reducing agent such as sodium borohydride can not reduce it alone (Ali et al., 2018a; Khalil et al., 2020). In the reduced form, the compound 4-Aminophenol, is extensively used in the synthesis of different drug compounds such as analgesic and antipyretic (Kamal et al., 2017b; Khan et al., 2019b). Therefore, from the industrial point of view, its reduction is also important which is usually achieved using a suitable catalyst. Metal nanoparticles such as gold, copper, silver, palladium and ruthenium facilitates this catalytic process easily (Kamal et al., 2018; Krajczewski et al., 2016). Oxides of some metals have been used for this type of conversion where they are used as catalysts (Khalil et al., 2020). It has been found that despite their important role in role in the catalytic reactions, nano-sized particles readily agglomerate with time due to their high surface energy thereby decreasing their efficiency (Favela-Camacho et al., 2019). Due to this reason, nanoparticles are tested in chemical reactions by using some sort of solid supports (Anwar and Alghamdi, 2020; Chen et al., 2015). Among different supports, zeolites, polymeric supports such as fibers, nanofibers, clay, filter papers and other materials have been used (Chen et al., 2015; Haider et al., 2018; Kamal et al.,

2016b; Yousefi et al., 2013). The use of these supports also aids in successful quantitative recovery of the catalyst from the reaction for the recyclability. In this regard, we aim at green biological synthesis route of highly active gold nanoparticles supported on cotton fabric.

The advantages of biological synthesis route of preparation of nanoparticles are: (1) no poisonous components, (2) no harsh conditions and, (3) no poisonous organic solvent (Ahmed et al., 2016b; Awad et al., 2019). Moreover, the developed nanoparticles coated cotton fabric was to develop a supported catalyst. Nanoparticles of different metals are well known for their catalytic performance in different reactions. In-fact, bare nanoparticles possess high surface to volume ratio (Baig et al., 2020; Das et al., 2019; He et al., 2015), which contributes to their high performance. However, due to their very small structures, nanoparticles recovery and re-use is not so effective (Ali et al., 2017a; Khan et al., 2018a; Zhang et al., 2018). Therefore, supported catalysts were introduced to ease the nanoparticles separation.

In this article, we have attempted to synthesize gold metal nanoparticles (AuNP) on cotton cloth (CC) surface using green chemistry approach. A fruit juice of commonly available plant of *Citrus limon* was used as green reductive and stabilizing component for the Au nanoparticles synthesis. The AuNP-CC was characterized and tested for catalytic and antibacterial application. The catalytic applications of AuNP-CC were performed on the reduction of nitrophenols and antibacterial applications were performed against human pathogenic gram-negative *Escherichia coli* and gram-positive *Staphylococcus aureus* bacterial strains.

2. Experimental

2.1. Materials

Cotton cloth was purchased from a local market. Tetrachloroauric (III) acid trihydrate ($\text{HAuCl}_4 \cdot 3\text{H}_2\text{O}$, > 99%), *p*-nitrophenol (>99%), *o*-nitrophenol (>99%) and sodium borohydride (NaBH_4 > 98%) were purchased from Sigma Aldrich. All the chemicals were of analytical grade reagents and used without further purification. De-ionized water was used in these experiments because the presence of other ions may interfere with the results.

2.2. Green synthetic approach to the AuNP-CC

Fresh *Citrus limon* was obtained from local market of Jeddah city, Saudi Arabia. After proper washing, they were cut into halves. The halves were subjected to mechanical press where its juice was extracted. The juice was filtered to separate the pulp particles from it. The juice was slightly heated to temperature not exceeding than 80 °C. This way the juice was concentrated and stored for further use in the synthesis of the metal nanoparticles.

Au nanoparticles (AuNPs) were synthesized using *Citrus limon* fruit extract by using HAuCl_4 salt aqueous solutions. Briefly, a cotton cloth (CC) was washed with a detergent using warm water followed by rinsing with deionized water. The CC was dipped in a 0.32 mM HAuCl_4 aqueous solution for 10 min at room temperature. Then 2 mL of extract was added to this system and solution was left at stirring. The CC was incubated

in an Au salt + extract mixed solution for 2 h at 30 °C. A visual change in color indicated the formation of the AuNPs on the CC. The AuNPs coated CC (AuNPs-CC) was removed from the precursor solution, washed with deionized water and lastly dried in the vacuum oven. The samples were stored for further experiments.

2.3. Catalytic testing of the AuNPs-CC

The green-route synthesized Au nanoparticles coated cotton cloth pieces were tested for two purposes. Their antimicrobial and catalytic properties were revealed. In the catalytic experiments, *p*-nitrophenol and *o*-nitrophenol were used as model pollutants. We briefly provide a catalytic experiment detail as below.

To a beaker containing 30 mL of either of the nitrophenol aqueous solution (0.09 mM), a freshly prepared NaBH₄ solution (1 mL of 3.5 M) was added. The mixed solution was continuously stirred. Subsequently, a desired amount of the AuNPs-CC was added to this solution. Absorption spectra were continuously recorded from this solution in a range of wavelength or at λ_{\max} position of *p*-NP and *o*-NP to observe the changes. A minimum of 2 min of time was given between each measurement. The absorbance values recorded by spectrophotometer were used in data analysis.

2.4. Antimicrobial studies

The antimicrobial activity of synthesized Au nanoparticles was evaluated by Kirby-Bauer disk diffusion method against human pathogenic gram-positive *Staphylococcus aureus* ATCC 25953 (*S. aureus*) and gram-negative *Escherichia coli* ATCC 25922 (*E. coli*) bacterial strains as reported in ref (Muthukumar et al., 2016, p. 7).

Nutrient agar is a common and widely used medium which was prepared in this study. For its preparation, ~28 g of nutrient agar powder was dissolved in 1L of deionized water. Then, it was autoclaved and poured in petri plates. Afterwards, the solidified media was incubated at 37 °C for 24 h to check any contamination. Then uncontaminated nutrient agar plates were taken and labelled with respect to strain and particles. For the preparation of inoculum, small amount of respective pathogenic strain was picked with sterile wire loop and suspended in 5 mL autoclaved nutrient broth and tubes kept for 24 h in shaking incubator for growth of microbes.

The turbidness of the prepared suspensions was attendant with 0.5 McFarland standard for standardized analysis. Afterwards, a standardized concentration of the test organisms was swabbed on agar plates and then cotton cloth (1 cm) containing an Au nanoparticles, 1 cm cloth with out AuNPs (negative control) and antibiotic drug (ampicillin) (positive control), respectively, were placed on the lawn of bacteria. The plates were carefully placed in an incubator at 37 °C for overnight. Generally, antimicrobial agent diffuses through the media and inhibit the growth of test microbes. As a result of this diffusion, a clear area around the samples, recognized as zone of inhibition, was measured on next day.

2.5. Characterization

Field emission scanning electron microscope (FESEM) was used for the surface analysis and studying the morphologies

of the prepared plant extract mediated Au metal nanoparticles as well as cotton cloth coated with these nanoparticles. In this study, both high and low magnification SEM images were acquired from the samples. The FESEM instrument was operated at high voltage. X-ray diffraction (XRD) experiments were performed to confirm the successful preparation of the nanoparticles and to know the crystalline nature of the nanoparticles or their impurities present in the samples. Thermoscientifics', ARL X'tra instrument was operated at high accelerating voltage to produce k-alpha radiations from copper anode. X-ray photoelectron spectroscopy analysis was performed using PHI5000 VersaProbeII, with maximum analysis depth of 10 nm under high vacuum (10⁻⁶). An inductively coupling plasma atomic emission spectrometer (ICP-AES, Optima 4100, USA) instrument was used to determine the metal content in the AuNP-CC sample. All the UV-visible spectroscopy experiments in this research work were performed on a Hitachi U3900 UV-Vis spectrophotometer.

3. Results and discussion

Fig. 1 shows the green synthetic steps involved in the preparation of AuNP-CC. It shows the extraction of *citrus limon* juice in a first step. Then it was mixed with CC and 0.08 HAuCl₄ and system temperature was raised. After maintaining the *Citrus limon* + HAuCl₄ + CC in a single pot under stirring for 2 h, a ruby red color was observed. The CC was further retained in the solution for 24 h for the maximum AuNP binding to its surface as -OH functional groups of cellulose macromolecules of CC can interact with it (Shankar et al., 2018). It was also observed that the reduction of the Au ions to nanoparticles by bare-CC was quite slow and necessarily needed a reductant. Fig. 2b shows the photographs of the samples in which left, middle and right represents the pristine, extract coated and AuNP-coated cotton cloth, respectively. The CC attained a color due to the attachment of the AuNP to its surface.

3.1. FESEM

Fig. 2 shows the surface morphology of two different CC samples. The neat CC's surface revealed that the sample was composed of woven fibers (Fig. 2a) while the individual fiber surface was smooth without any attachment of particles (Fig. 2b). On the other hand, the AuNP-CC's surface was not smooth as shown in highly magnified SEM image shown in Fig. 2d. The presence of bright nanoparticles can be clearly seen in this image. This represents the attachment of the AuNP to the CC's fiber surface. The average particle size was ~22 nm. The AuNPs content attached to the CC fibers was 1.82×10^{-5} mol per 100 mg of substrate as measured by ICP-AES method.

3.2. XPS and XRD

Fig. 3a shows the XPS survey scans of pristine-CC and AuNPs-CC in which major peaks of C 1s and O 1s in pristine-CC were labelled. In addition to these peaks, small peaks of Au element were identified in the XPS spectrum of AuNPs-CC sample. Fig. 3b shows the high resolution XPS spectrum of AuNPs-CC in the range of 79.5–88.2 eV. Two

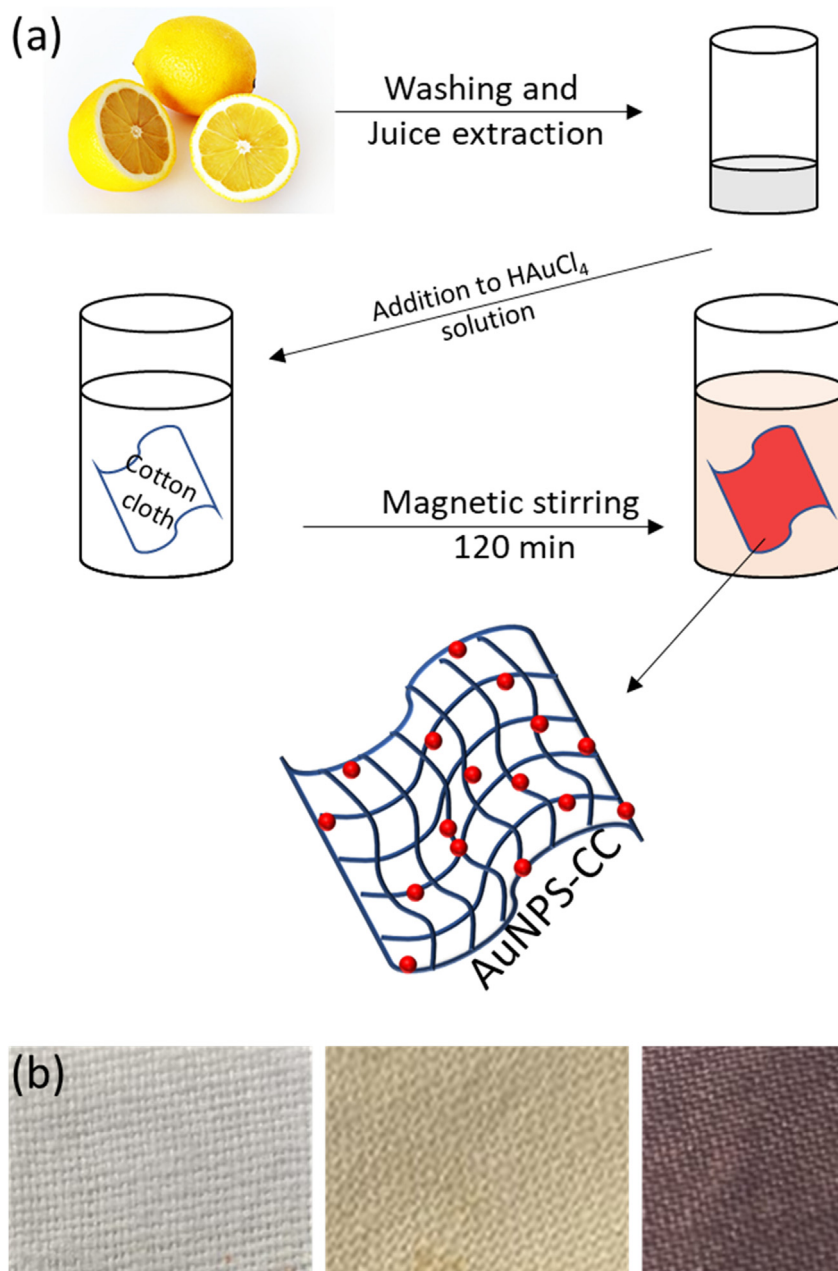


Fig. 1 Illustration of green synthetic approach towards AuNP-CC preparation (a), and photographs of the (b) bare-CC (left), extract coated-CC (middle) and AuNP-CC (right).

clear peaks at 82.2 and 85.7 eV could be observed which represents the binding energies of 4f_{7/2} and 4f_{5/2} of Au metal. Such results signify that AuNPs were deposited on the CC fibers during currently adopted green synthesis method. Fig. 3c shows the XRD profiles of the two samples, in which, the XRD profile of pure CC showed diffraction peaks at $2\theta = 15^\circ, 16.8^\circ, 22.9^\circ$ and 34.5° . The same peaks were also observed in the XRD profile of the AuNPs-CC. These diffractions represent the crystalline nature of the CC due to cellulose crystals (Venkateswara Rao et al., 2019). Moreover, a weak diffraction peaks at $2\theta = 38.5^\circ$ for Au-metal was also observed in the AuNPs-CC sample (Khan et al., 2018b).

4. Catalytic testing

The toxicity of water due to nitrophenols can be minimized by reducing it to the less-toxic aminophenols (Wang et al., 2020). This reduction is usually carried out with the NaBH₄ as shown in Fig. 4. We first tested the bare supports as catalysts in the nitrophenols transformation as the data are shown in Figure SI-1. No catalytic activity for the reduction of both the nitrophenols was observed upon using a substrate only as a catalyst. To our delight, the reduction of *p*- and *o*-NP occurred rapidly in the presence of AuNPs-CC catalyst. The successful reactions were confirmed by UV-visible spectra

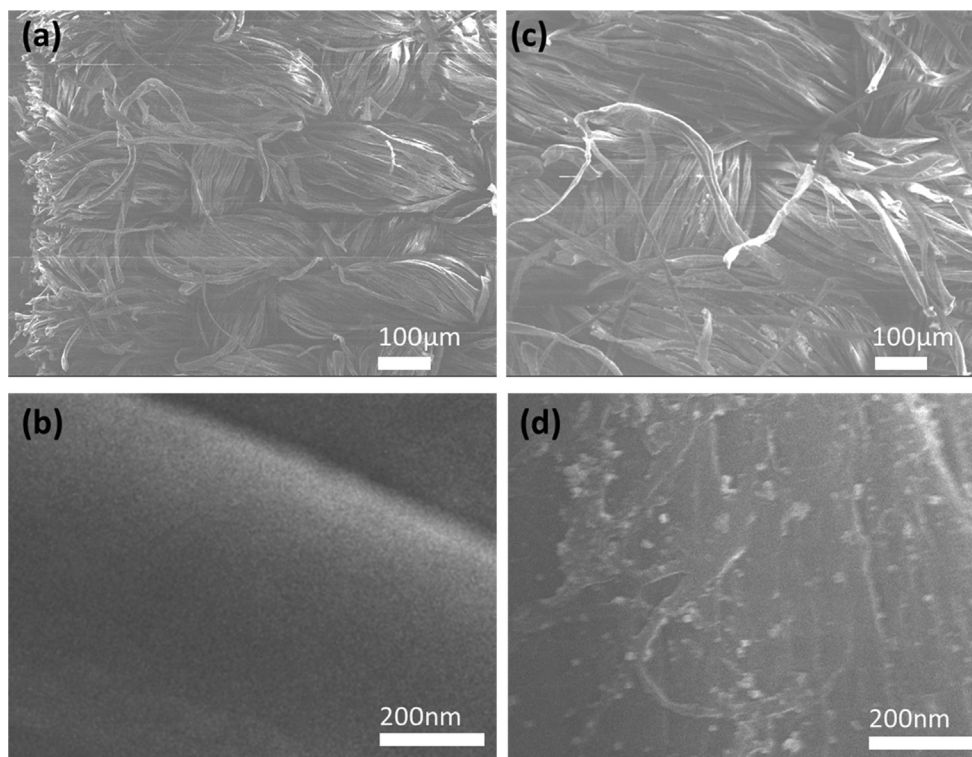


Fig. 2 FESEM images of (a,b) bare cotton cloth and (c,d) AuNP-CC.

shown in Fig. 5. Some major conversion steps of *p*-NP reduction process were shown by (Al-Ghamdi and Khan, 2020).

Fig. 5a shows that the peak at 400 nm started to decrease with time. The time taken for its complete disappearance was 32 min and another new peak appearance was also observed at a location of 290. The color of the solution was changed from light to bright yellow with the addition of the reducing agent indicating that the *p*-NPA was formed. *p*-NPA was very stable as the peak at 400 nm had the same intensity even after 2 h. It implies that NaBH_4 alone was unable to reduce the *p*-NP. The changes observed during the passage of time after addition of the catalyst indicate that *p*-AP was formed. It is clear from some reports that the *p*-NP to *p*-AP conversion is an atom economic reaction. This is due to the straight-forward formation of a single product as revealed by Guo *et al* in the GC-MS analysis (Guo *et al.*, 2016). Another important reduction reaction was also studied here. Fig. 5b shows the UV-vis spectra of *o*-NP solution during its reduction. The spectra were successively recorded with 4 min interval. It can be seen in this figure that the peak at 415 nm decreased with time. Such a decrease in this peak was regarded to the successfully formation of the *o*-AP as reported by (Khan *et al.*, 2019a).

4.1. Effect of catalyst dose and concentration of nitrophenol

To study the reaction kinetics, the *pseudo-first order* kinetics equation was used. It is given as follow,

$$\ln(A_t) = -kt + \ln(A_0)$$

in which, A_0 is initial absorbance value, A_t is absorbance at time t and k is the rate constant.

The k value can be determined from the experimental absorption spectroscopy data.

Fig. 6 shows the plot of $\ln(A_t/A_0)$ vs time (min) for the nitrophenols reduction which shows a linear connection. This indicates that both the reduction reactions followed the pseudo-first order kinetics. The k was calculated to be 0.109 min^{-1} and 0.063 min^{-1} for *p*-NP and *o*-NP, respectively. Furthermore, the effect of reactant concentrations as well as the catalyst dosage on the k was studied. Fig. 6a shows the plot of $\ln(A_t/A_0)$ vs time for the *p*-NP reduction where reactants concentration was changed. It is clear from this figure that the k value increased with the decreasing *p*-NP concentration at constant catalyst amount this figure that the k value increased with the decreasing *p*-NP concentration at constant catalyst amount. The k values for 0.06 mM, 0.09 mM and 0.15 mM of *p*-NP were 0.156 min^{-1} , 0.109 min^{-1} and 0.069 min^{-1} , respectively. Similarly, Fig. 6b shows the plot of $\ln(A_t/A_0)$ vs time for the *o*-NP reduction and the k values for 0.06 mM, 0.09 mM and 0.15 mM *o*-NP were 0.108 min^{-1} , 0.063 min^{-1} and 0.042 min^{-1} , respectively. In a similar way, (Khan *et al.*, 2019a) used a Cu/CH-PUS catalyst in three different reactions where concentration of *p*-NP was changed. They also detected a similar trend of decrease in k upon increasing the reactants concentration.

Fig. 7a and b shows the effect of AuNPs-CC catalyst dosage on the k of the *p*-NP and *o*-NP reduction. It is evident from this figure that the k increased for both reduction reactions with increasing amount of the catalyst which supported the results of ref (Khan *et al.*, 2019a). The catalyst amount was varied between 6 and 20 mg. As clear from Fig. 7a, the k of 0.139 min^{-1} , 0.109 min^{-1} , 0.085 min^{-1} and 0.037 min^{-1} was obtained for *p*-NP by using a 20 mg, 15 mg 10 mg and

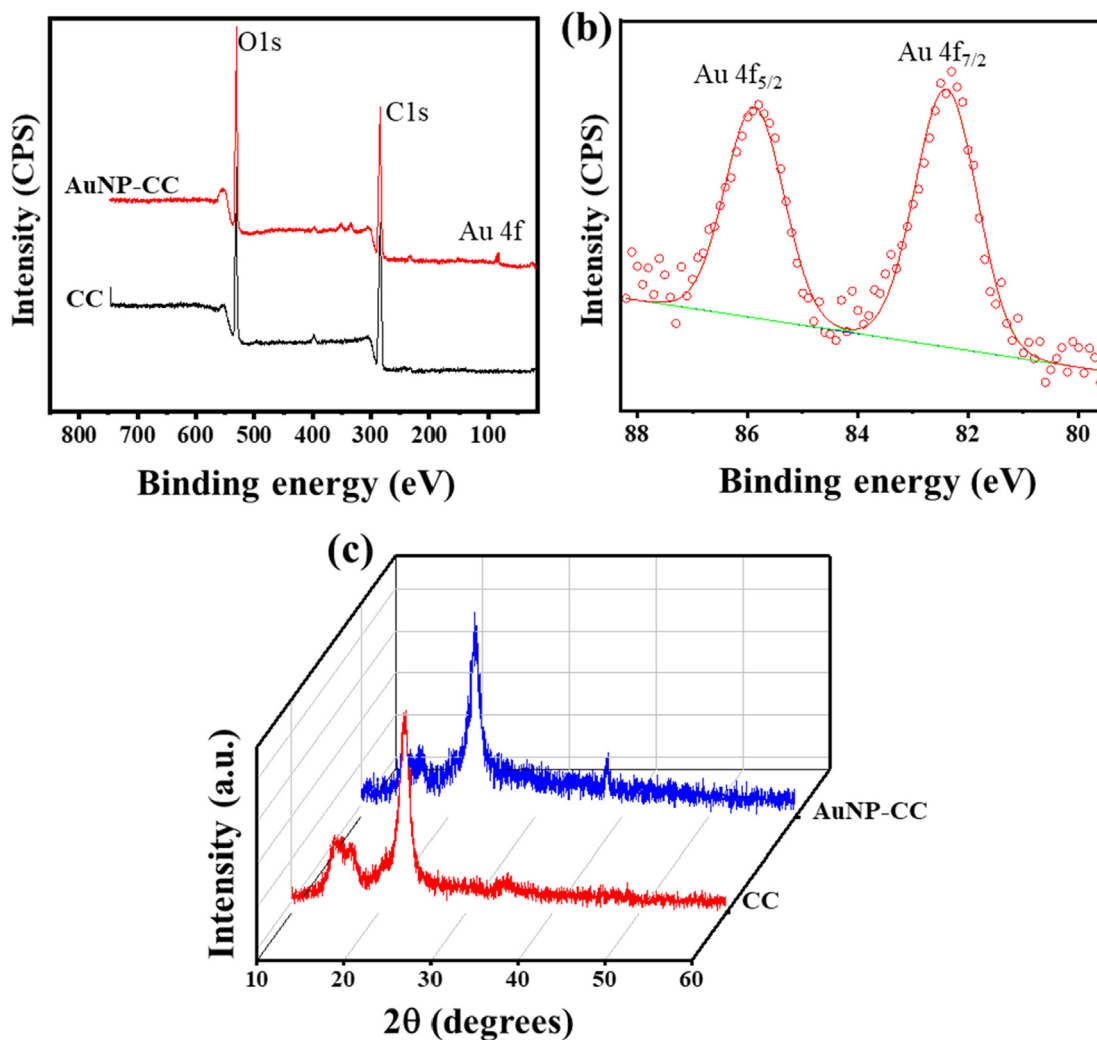


Fig. 3 XPS survey scan (a) of CC and AuNPs-CC and (b) high resolution scan of AuNPs-CC in the range of 80–89 eV, and (c) XRD profiles of the two samples.

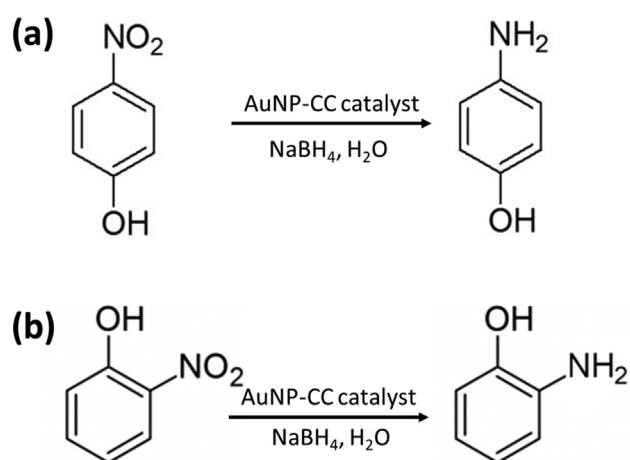


Fig. 4 Typical transformation reactions of (a) p-NP and (b) o-NP.

6 mg, respectively. The k of 0.091 min^{-1} , 0.063 min^{-1} , 0.053 min^{-1} and 0.032 min^{-1} was obtained for *o*-NP by using a 20 mg, 15 mg 10 mg and 6 mg, respectively. Similar to our study, (Gopiraman et al., 2020) reported the increasing amount of the catalyst (Rh-nanoparticles anchored on onion-like fullerene) effect on the k . They found an increase in the k value with the increase in the catalyst dosage. Moreover, (Ismail et al., 2018) prepared plant supported Cu-Ag and Cu-Ni bimetallic nanoparticles and used it for the reduction of different nitrophenols as well as dye pollutants. Their results were promising and reported trends similar to our study.

4.2. Cotton cloth supported Au nanoparticles

Due to difficulties in recovery of the spent catalyst, the use of Au nanoparticles-based catalyst at industrial scale is highly limited. Au nanoparticles, similar to other metal nanoparticles, have been loaded on magnetic substrates for easy recovery.

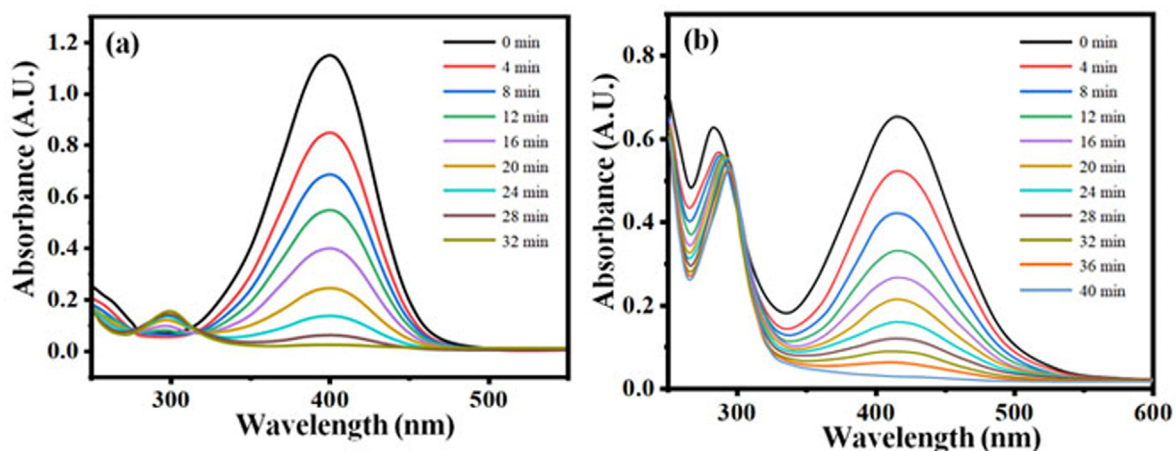


Fig. 5 Typical UV-visible spectra of (a) p-NP and (b) o-NP during their reduction using the AuNP-CC catalyst.

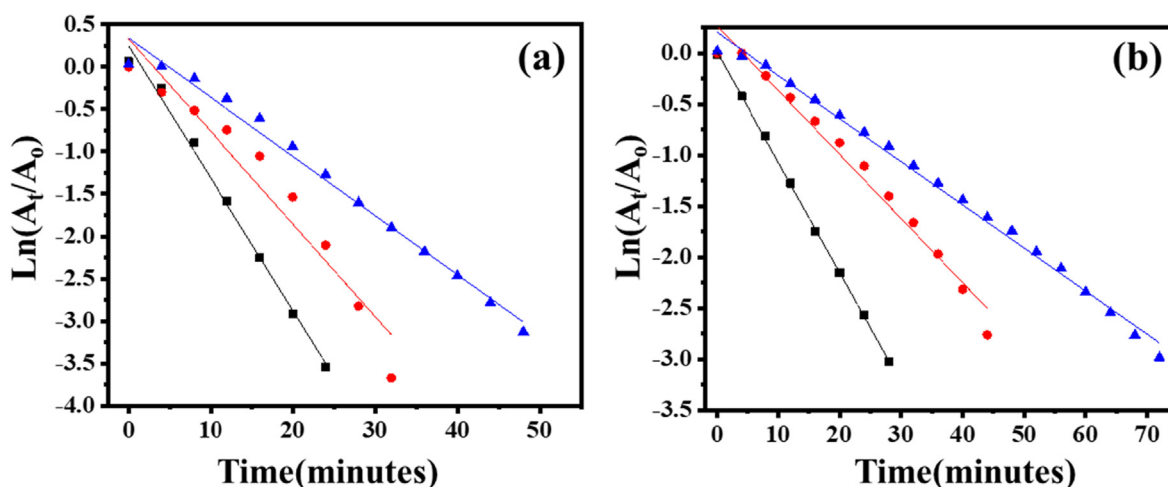


Fig. 6 Plot of $\ln(A_t/A_0)$ vs time (min) for p-NP and (b) o-NP while changing their initial concentration. \blacksquare = 0.06 mM, \bullet = 0.09 mM and \blacktriangle = 0.15 mM of nitrophenols aqueous solution.

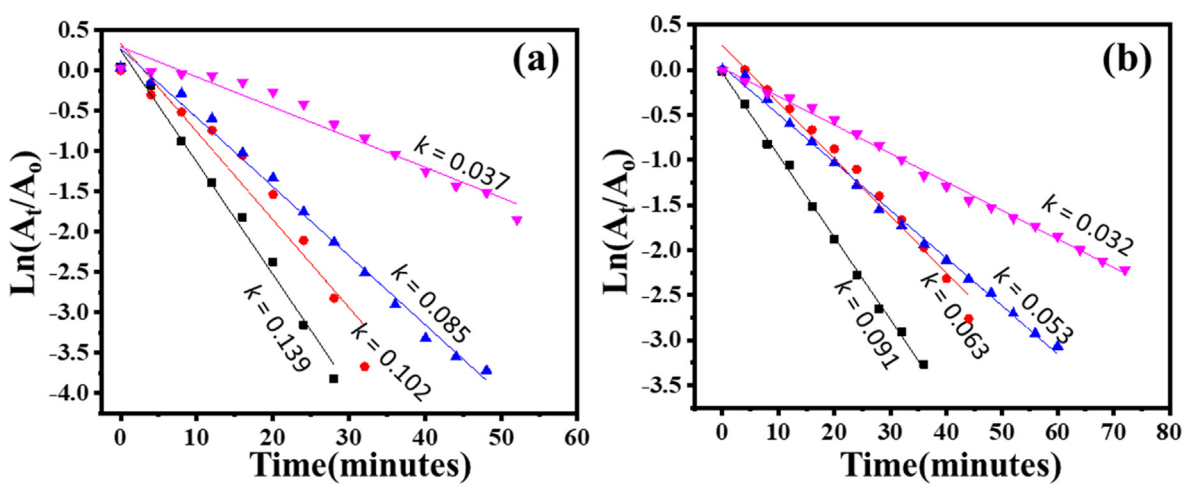


Fig. 7 Plot of $\ln(A_t/A_0)$ vs time (min) for p-NP and (b) o-NP while changing the catalyst dosage.

Moreover, Au nanoparticles-based catalysts are often recovered through centrifuge process for another batch of reaction which is time-consuming. In order to abstain the aggregation and easy recovery, Au nanoparticles could be loaded on different supports. As stated in literature by researchers, polysaccharide-based supports (chitosan, cellulose, filter paper etc.) are best for this purpose. Previously, noble metal nanoparticles (Ag and Au) loaded on filter paper/cellulose acetate sheets were demonstrated for SERS and sensor applications (Ahmad et al., 2016; Kamal et al., 2017a; Khan et al., 2017; Zheng et al., 2015). Some researchers used binders of polyethyleneimine, polydopamine, agar, and chitosan to adhere the nanoparticles to the substrate surface. In this study, the Au nanoparticles adhered to cotton cloth was utilized as catalyst in a fixed-bed type reactor. Such reactor is superior to convention batch type reactors. In their study, a fixed-bed type reactor for the pollutants reduction was used while using the Ca-alginate nanocomposite beads as catalyst (Marwani and Ahmad, 2020). Similarly, Gao et al used silver/lignin/polyacrylic acid hydrogel catalyst in fixed-bed type reactor for the pollutants reduction and reported the high stability of their catalyst (Gao et al., 2020). A similar type of experimental setup, for the continuous flow fixed-bed type reactor consisting of a burette clamped on a stand with the AuNPs-cotton cloth placed at its bottom, has been shown by (Marwani and Ahmad, 2020). In their study, a fixed-bed type reactor for the pollutants reduction was used while using the Ca-alginate nanocomposite beads as catalyst (Marwani and Ahmad, 2020). Similarly, Gao et al used silver/lignin/polyacrylic acid hydrogel catalyst in fixed-bed type reactor for the pollutants reduction and reported the high stability of their catalyst (Gao et al., 2020). In our experimental study, *p*-NP or *o*-NP aqueous solution mixed with the NaBH_4 was passed through it. The solution obtained at the bottom of the burette was analyzed by spectrophotometer. Fig. 8a shows the UV-vis spectra of the *p*-NP and *o*-NP solutions before and after passing it through this setup. It can be seen in Fig. 8b that more than 90% reduction of the nitrophenols happened through this procedure after passing the 12 solution batches.

5. Antibacterial properties

The bactericidal features of cotton based composites are establishing new dimension in their medical, pharmaceutical, packaging and other applications (Anwar and Alghamdi, 2020; Ganesan and Gurumallesh Prabu, 2019). Pure cellulose is a non toxic material thus lacking any antimicrobial feature. On other hand the bactericidal nature of most of the nanoparticles is well known. NPs have been effectively utilized in treatment of many diseases caused by bacteria and viruses (Tsai et al., 2017). The very small size of NPs enable them to penetrate in the microbial body and destroy it through different reported mechanisms (Kavitha et al., 2017). Together with impressive antimicrobial features of pure NPs, it worth mentioning that NPs retain their antimicrobial features even if combined in the form of composites with polymers and other materials.

Considering the potential applications of cotton based materials in wound dressing, facial masks, biomedical instruments, drug storage and carrying equipment, it is imperative to impregnate these with antimicrobial features. Currently synthesized Au NPs-CC composites were therefore expected to exhibit antibacterial activities. The antimicrobial properties shown in Fig. 9 were evaluated against model gram negative (*E. coli*) and gram positive (*S. aureus*) pathogenic strains in comparison to negative control (cotton) and positive control (model drug). The antibacterial results shown in Fig. 9 indicated that the green synthesized AuNPs-CC samples exhibited a clear inhibitory zone against both *E. coli* and *S. aureus* species. The average inhibitory zone obtained for sample was 16 mm and 18 mm against *E. coli* and *S. aureus*, respectively, compared to 40 mm and zero of positive and negative control against both species. These results are highly satisfactory and providing vital clues that the green synthesized AuNPs-CC composites can be effectively utilized for microbial disinfection together with other targeted applications.

As reported by (Velmurugan et al., 2016), pure AuNPs do not possess adequately the ability to kill bacteria, however, green-synthesized AuNPs are shown to possess antibacterial

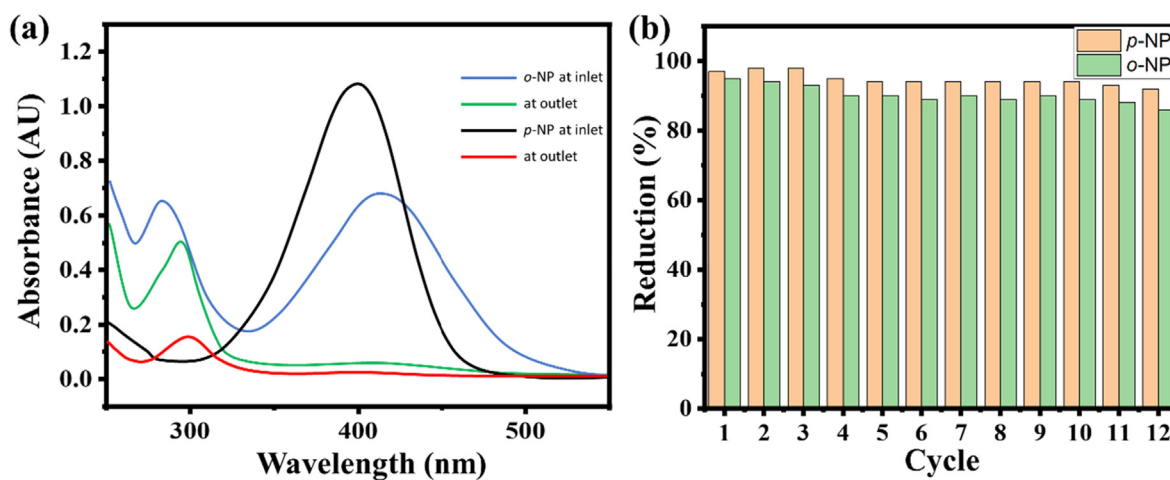


Fig. 8 UV-visible spectra of (a) nitrophenols at inlet and outlet of the burette while passing it through an AuNPs-CC and (b) their reduction percentage during six cycles.

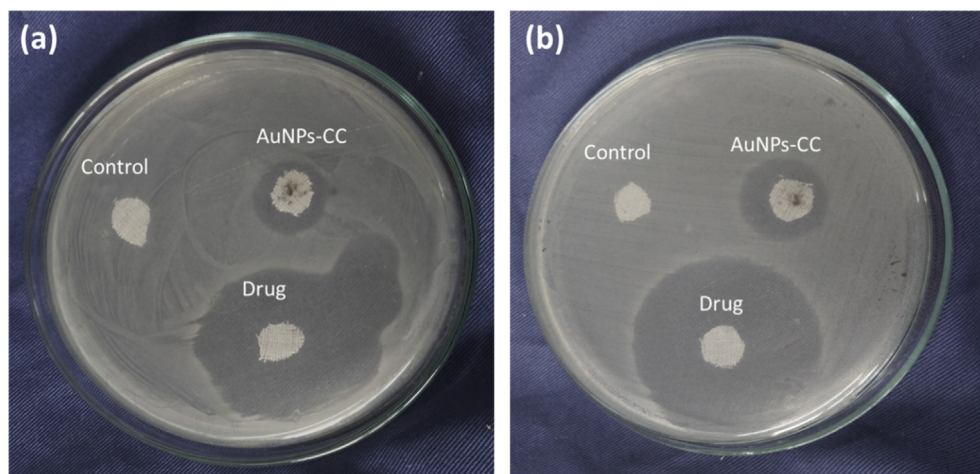


Fig. 9 Inhibition zones of green synthesized AuNPs-CC, positive control (drug) and negative control (CC) against (a) *E. coli* and (b) *S. aureus* after incubation for 24 h.

activities which arise from the plant extract components found on the surface of samples. Moreover, previously it has been shown that the *Citrus limon* juice has antibacterial effects (Otang and Afolayan, 2016), and therefore, the antibacterial properties observed here may be due to the some active components of the juice concentrate. The bactericidal effects observed in our studies are in accordance with previously published literature (Shan et al., 2019; Tsai et al., 2017). A small difference in the bactericidal activities against both pathogens could be attributed to the difference in their cell wall structure (Shan et al., 2019).

6. Conclusions

Gold nanoparticles were successfully prepared using a green biological synthetic approach where a *Citrus limon* juice was used as reductant for the tri-valent Au ionic solution. Further, a cotton cloth surface was functionalized with the prepared AuNP. The AuNP-CC was tested in the two important reduction reactions of nitrophenols where highest reaction rates of 0.139 and 0.091 min⁻¹ were observed in batch type reaction. The AuNP-CC was also efficient in catalyzing the nitrophenols in fixed-bed type reactor where a continuous flow of these solutions was achieved with high conversion of above 90%. Moreover, the AuNP-CC catalyst maintained high catalytic activity during recycle operation. This proved that the CC guaranteed the best carrier to the AuNP. Furthermore, the AuNP-CC also successfully inhibited the *E. coli* and *S. aureus* growth.

Declaration of Competing Interest

The authors declare that they have no known competing financial interests or personal relationships that could have appeared to influence the work reported in this paper.

Acknowledgement

This work was supported by the Deanship of Scientific Research (DSR), King Abdulaziz University, Jeddah under

grant No. (D-205-130-1439). The authors, therefore, gratefully acknowledge the DSR technical and financial support.

Appendix A. Supplementary material

Supplementary data to this article can be found online at <https://doi.org/10.1016/j.arabjc.2021.103327>.

References

- Ahmad, I., Kamal, T., Khan, S.B., Asiri, A.M., 2016. An efficient and easily retrievable dip catalyst based on silver nanoparticles/chitosan-coated cellulose filter paper. *Cellulose* 23, 3577–3588. <https://doi.org/10.1007/s10570-016-1053-4>.
- Ahmed, M.S., Kamal, T., Khan, S.A., Anwar, Y., Saeed, M.T., Asiri, A.M., Khan, S.B., 2016a. Assessment of anti-bacterial Ni-Al/chitosan composite spheres for adsorption assisted photo-degradation of organic pollutants. *Curr. Nanosci.* 12, 569–575. <https://doi.org/10.2174/1573413712666160204000517>.
- Ahmed, S., Ahmad, M., Swami, B.L., Ikram, S., 2016b. A review on plants extract mediated synthesis of silver nanoparticles for antimicrobial applications: a green expertise. *J. Adv. Res.* 7, 17–28.
- Al-Ghamdi, Y.O., Khan, S.A., 2020. Stabilization of zero-valent Au nanoparticles on carboxymethyl cellulose layer coated on chitosan-CBV 780 zeolite Y sheets: assessment in the reduction of 4-nitrophenol and dyes. *Cellulose* 27, 8827–8841. <https://doi.org/10.1007/s10570-020-03379-0>.
- Ali, F., Khan, S.B., Kamal, T., Alamry, K.A., Asiri, A.M., Sobahi, T.R.A., 2017a. Chitosan coated cotton cloth supported zero-valent nanoparticles: simple but economically viable, efficient and easily retrievable catalysts. *Sci. Rep.* 7, 16957. <https://doi.org/10.1038/s41598-017-16815-2>.
- Ali, F., Khan, S.B., Kamal, T., Alamry, K.A., Bakhsh, E.M., Asiri, A.M., Sobahi, T.R.A., 2018a. Synthesis and characterization of metal nanoparticles templated chitosan-SiO₂ catalyst for the reduction of nitrophenols and dyes. *Carbohydr. Polym.* 192, 217–230. <https://doi.org/10.1016/j.carbpol.2018.03.029>.
- Ali, F., Khan, S.B., Kamal, T., Anwar, Y., Alamry, K.A., Asiri, A.M., 2017b. Bactericidal and catalytic performance of green nanocomposite based on chitosan/carbon black fiber supported monometallic and bimetallic nanoparticles. *Chemosphere* 188, 588–598. <https://doi.org/10.1016/j.chemosphere.2017.08.118>.

- Ali, N., Awais, Kamal, T., Ul-Islam, M., Khan, A., Shah, S.J., Zada, A., 2018b. Chitosan-coated cotton cloth supported copper nanoparticles for toxic dye reduction. *Int. J. Biol. Macromol.* 111, 832–838. <https://doi.org/10.1016/j.ijbiomac.2018.01.092>.
- Ali, N., Azeem, S., Khan, A., Khan, H., Kamal, T., Asiri, A.M., 2020a. Experimental studies on removal of arsenites from industrial effluents using tridodecylamine supported liquid membrane. *Environ Sci Pollut Res* 27, 11932–11943. <https://doi.org/10.1007/s11356-020-07619-5>.
- Ali, N., Khan, A., Riaz, A., Asiri, A.M., Kamal, T., 2020b. Photocatalytic performance evaluation of bismuth doped tin-dioxide under uv and direct sunlight irradiation for congo red dye degradation. *J. Chem. Soc. Pak.* 42, 687–695.
- Ali, N., Khan, A., Riaz, A., Kamal, A.M.A., T., 2020c. Photocatalytic Performance evaluation of bismuth doped tin-dioxide under UV and direct sunlight irradiation for congo red dye degradation. *JCSP* 42, 687.
- Ali, Y., Ahmad, B., Alghamdi, K.M., Kamal, T., Ali, H.S.H.M., Anwar, Y., Hussain, A., Jomezai, N.U., 2019. Characterization of recombinant cold active lipase from a novel *Pseudomonas* spp. MG687270. *Int. J. Agric. Biol.* 22, 855–865. <https://doi.org/10.17957/IJAB/15.1141>.
- Anwar, Y., 2018. Antibacterial and lead ions adsorption characteristics of chitosan-manganese dioxide bionanocomposite. *Int. J. Biol. Macromol.* 111, 1140–1145. <https://doi.org/10.1016/j.ijbiomac.2018.01.096>.
- Anwar, Y., Alghamdi, K.M., 2020. Imparting antibacterial, antifungal and catalytic properties to cotton cloth surface via green route. *Polym. Test.* 81, <https://doi.org/10.1016/j.polymertesting.2019.106258> 106258.
- Awad, M.A., Eisa, N.E., Virk, Promy, Hendi, A.A., Ortashi, K.M.O. O., Mahgoub, A.S.A., Elobeid, M.A., Eissa, F.Z., 2019. Green synthesis of gold nanoparticles: Preparation, characterization, cytotoxicity, and anti-bacterial activities. *Mater. Lett.* 256, <https://doi.org/10.1016/j.matlet.2019.126608> 126608.
- Baig, M.M., Pervaiz, E., Afzal, M.J., 2020. Catalytic activity and kinetic studies of Core@Shell nanostructure NiFe₂O₄@TiO₂ for photocatalytic degradation of methyl orange dye. *J. Chem. Soc. Pak.* 42, 531–541.
- Cerkez, I., Kocer, H.B., Worley, S.D., Broughton, R.M., Huang, T.S., 2012. N-halamine copolymers for biocidal coatings. *React. Funct. Polym.* 72, 673–679. <https://doi.org/10.1016/j.reactfunctpolym.2012.06.018>.
- Ceylan, Z., Aydin, S.D., 2020. Investigation of the effect of substituent species/positions and numbers on removal of toxicity from chloro and nitro phenol compounds with fenton and fenton-like processes. *J. Chem. Soc. Pak.* 42, 504–514.
- Chen, M., Kang, H., Gong, Y., Guo, J., Zhang, H., Liu, R., 2015. Bacterial cellulose supported gold nanoparticles with excellent catalytic properties. *ACS Appl. Mater. Interfaces* 7, 21717–21726. <https://doi.org/10.1021/acsami.5b07150>.
- Das, R., Sypu, V.S., Paumo, H.K., Bhaumik, M., Maharaj, V., Maity, A., 2019. Silver decorated magnetic nanocomposite (Fe₃O₄@PPy-MAA/Ag) as highly active catalyst towards reduction of 4-nitrophenol and toxic organic dyes. *Appl. Catal. B* 244, 546–558. <https://doi.org/10.1016/j.apcatb.2018.11.073>.
- Favela-Camacho, S.E., Samaniego-Benítez, E.J., Godínez-García, A., Avilés-Arellano, L.Ma., Pérez-Robles, J.F., 2019. How to decrease the agglomeration of magnetite nanoparticles and increase their stability using surface properties. *Colloids Surf., A* 574, 29–35. <https://doi.org/10.1016/j.colsurfa.2019.04.016>.
- Ganesan, R.M., Gurumallesh Prabu, H., 2019. Synthesis of gold nanoparticles using herbal *Acorus calamus* rhizome extract and coating on cotton fabric for antibacterial and UV blocking applications. *Arabian J. Chem.* 12, 2166–2174. <https://doi.org/10.1016/j.arabjc.2014.12.017>.
- Gao, C., Wang, X., Wang, H., Zhou, J., Zhai, S., An, Q., 2020. Highly efficient and stable catalysis of p-nitrophenol via silver/lignin/polyacrylic acid hydrogel. *Int. J. Biol. Macromol.* 144, 947–953. <https://doi.org/10.1016/j.ijbiomac.2019.09.172>.
- Gopiraman, M., Saravanamoorthy, S., Ullah, S., Ilangovan, A., Kim, I.S., Chung, I.M., 2020. Reducing-agent-free facile preparation of Rh-nanoparticles uniformly anchored on onion-like fullerene for catalytic applications. *RSC Adv.* 10, 2545–2559. <https://doi.org/10.1039/C9RA09244G>.
- Guo, P., Tang, L., Tang, J., Zeng, G., Huang, B., Dong, H., Zhang, Y., Zhou, Y., Deng, Y., Ma, L., Tan, S., 2016. Catalytic reduction-adsorption for removal of p-nitrophenol and its conversion p-aminophenol from water by gold nanoparticles supported on oxidized mesoporous carbon. *J. Colloid Interface Sci.* 469, 78–85. <https://doi.org/10.1016/j.jcis.2016.01.063>.
- Haider, A., Haider, S., Kang, I.-K., Kumar, A., Kumara, M.R., Kamal, T., Han, S.S., 2018. A novel use of cellulose based filter paper containing silver nanoparticles for its potential application as wound dressing agent. *Int. J. Biol. Macromol.* 108, 455–461. <https://doi.org/10.1016/j.ijbiomac.2017.12.022>.
- He, Y., Huang, G., Pan, Z., Liu, Y., Gong, Q., Yao, C., Gao, J., 2015. Polyelectrolyte induced formation of silver nanoparticles in copolymer hydrogel and their application as catalyst. *Mater. Res. Bull.* 70, 263–271. <https://doi.org/10.1016/j.materresbull.2015.04.028>.
- Hou, A., Feng, G., Zhuo, J., Sun, G., 2015. UV light-induced generation of reactive oxygen species and antimicrobial properties of cellulose fabric modified by 3,3',4,4'-benzophenone tetracarboxylic acid. *ACS Appl. Mater. Interfaces* 7, 27918–27924. <https://doi.org/10.1021/acsami.5b09993>.
- Ismail, M., Khan, M.I., Khan, S.B., Khan, M.A., Akhtar, K., Asiri, A. M., 2018. Green synthesis of plant supported CuAg and CuNi bimetallic nanoparticles in the reduction of nitrophenols and organic dyes for water treatment. *J. Mol. Liq.* 260, 78–91. <https://doi.org/10.1016/j.molliq.2018.03.058>.
- Kamal, T., Ahmad, I., Khan, S.B., Asiri, A.M., 2018. Agar hydrogel supported metal nanoparticles catalyst for pollutants degradation in water. *Desalin. Water Treat.* 136, 290–298. <https://doi.org/10.5004/dwt.2018.23230>.
- Kamal, T., Ahmad, I., Khan, S.B., Asiri, A.M., 2017a. Synthesis and catalytic properties of silver nanoparticles supported on porous cellulose acetate sheets and wet-spun fibers. *Carbohydr. Polym.* 157, 294–302. <https://doi.org/10.1016/j.carbpol.2016.09.078>.
- Kamal, T., Khan, S.B., Asiri, A.M., 2016a. Nickel nanoparticles-chitosan composite coated cellulose filter paper: an efficient and easily recoverable dip-catalyst for pollutants degradation. *Environ. Pollut.* 218, 625–633. <https://doi.org/10.1016/j.envpol.2016.07.046>.
- Kamal, T., Khan, S.B., Asiri, A.M., 2016b. Synthesis of zero-valent Cu nanoparticles in the chitosan coating layer on cellulose microfibrils: evaluation of azo dyes catalytic reduction. *Cellulose* 23, 1911–1923. <https://doi.org/10.1007/s10570-016-0919-9>.
- Kamal, T., Khan, S.B., Haider, S., Alghamdi, Y.G., Asiri, A.M., 2017b. Thin layer chitosan-coated cellulose filter paper as substrate for immobilization of catalytic cobalt nanoparticles. *Int. J. Biol. Macromol.* 104, 56–62. <https://doi.org/10.1016/j.ijbiomac.2017.05.157>.
- Kavitha, T., Haider, S., Kamal, T., Ul-Islam, M., 2017. Thermal decomposition of metal complex precursor as route to the synthesis of Co₃O₄ nanoparticles: Antibacterial activity and mechanism. *J. Alloy. Compd.* 704, 296–302. <https://doi.org/10.1016/j.jallcom.2017.01.306>.
- Khalil, A., Ali, N., Khan, A., Asiri, A.M., Kamal, T., 2020. Catalytic potential of cobalt oxide and agar nanocomposite hydrogel for the chemical reduction of organic pollutants. *Int. J. Biol. Macromol.* 164, 2922–2930. <https://doi.org/10.1016/j.ijbiomac.2020.08.140>.
- Khan, F.U., Asimullah, Khan, S.B., Kamal, T., Asiri, A.M., Khan, I. U., Akhtar, K., 2017. Novel combination of zero-valent Cu and Ag nanoparticles @ cellulose acetate nanocomposite for the reduction of 4-nitro phenol. *Int. J. Biol. Macromol.* 102, 868–877. <https://doi.org/10.1016/j.ijbiomac.2017.04.062>.

- Khan, M.S.J., Kamal, T., Ali, F., Asiri, A.M., Khan, S.B., 2019a. Chitosan-coated polyurethane sponge supported metal nanoparticles for catalytic reduction of organic pollutants. *Int. J. Biol. Macromol.* 132, 772–783. <https://doi.org/10.1016/j.ijbiomac.2019.03.205>.
- Khan, M.S.J., Khan, S.B., Kamal, T., Asiri, A.M., 2019b. Agarose biopolymer coating on polyurethane sponge as host for catalytic silver metal nanoparticles. *Polym. Test.* 78, <https://doi.org/10.1016/j.polymertesting.2019.105983> 105983.
- Khan, S., Ul-Islam, M., Ikram, M., Islam, S.U., Ullah, M.W., Israr, M., Jang, J.H., Yoon, S., Park, J.K., 2018a. Preparation and structural characterization of surface modified microporous bacterial cellulose scaffolds: a potential material for skin regeneration applications *in vitro* and *in vivo*. *Int. J. Biol. Macromol.* 117, 1200–1210. <https://doi.org/10.1016/j.ijbiomac.2018.06.044>.
- Khan, S., Ul-Islam, M., Ullah, M.W., Israr, M., Jang, J.H., Park, J.K., 2018b. Nano-gold assisted highly conducting and biocompatible bacterial cellulose-PEDOT:PSS films for biology-device interface applications. *Int. J. Biol. Macromol.* 107, 865–873. <https://doi.org/10.1016/j.ijbiomac.2017.09.064>.
- Krajczewski, J., Kołataj, K., Kudelski, A., 2016. Enhanced catalytic activity of solid and hollow platinum-cobalt nanoparticles towards reduction of 4-nitrophenol. *Applied Surface Science, E-MRS 2015 Fall Meeting, Symposium D: “12th International Symposium on Electrochemical/Chemical Reactivity of New Materials (ECRNM 12) – Surface Science – key to understand advanced materials” 15th-18th September 2015, Warsaw, Poland* 388, 624–630. <https://doi.org/10.1016/j.apsusc.2016.04.089>.
- Martin, J.K., Sheehan, J.P., Bratton, B.P., Moore, G.M., Mateus, A., Li, S.H.-J., Kim, H., Rabinowitz, J.D., Typas, A., Savitski, M.M., Wilson, M.Z., Gitai, Z., 2020. A dual-mechanism antibiotic kills gram-negative bacteria and avoids drug resistance. *Cell* 181, 1518–1532.e14. <https://doi.org/10.1016/j.cell.2020.05.005>.
- Marwani, H.M., Ahmad, S., 2020. Efficient reduction of environmental pollutants using metal nanoparticles catalyst on calcium alginate surface. *Int. J. Environ. Anal. Chem.*, 1–17 <https://doi.org/10.1080/03067319.2020.1811258>.
- Muthukumar, T., Sudhakumari, Sambandam, B., Aravinthan, A., Sastry, T.P., Kim, J.-H., 2016. Green synthesis of gold nanoparticles and their enhanced synergistic antitumor activity using HepG2 and MCF7 cells and its antibacterial effects. *Process Biochem.* 51, 384–391. <https://doi.org/10.1016/j.procbio.2015.12.017>.
- Ng, I.-S., Ooi, C.W., Liu, B.-L., Peng, C.-T., Chiu, C.-Y., Chang, Y.-K., 2020. Antibacterial efficacy of chitosan- and poly(hexamethylene biguanide)-immobilized nanofiber membrane. *Int. J. Biol. Macromol.* 154, 844–854. <https://doi.org/10.1016/j.ijbiomac.2020.03.127>.
- Otang, W.M., Afolayan, A.J., 2016. Antimicrobial and antioxidant efficacy of Citrus limon L. peel extracts used for skin diseases by Xhosa tribe of Amathole District, Eastern Cape, South Africa. *S. Afr. J. Bot.* 102, 46–49. <https://doi.org/10.1016/j.sajb.2015.08.005>.
- Shan, M., Liu, C., Shi, L., Zhang, L., Lin, Y., Zhang, S., Zhu, Z., Wang, X., Zhuang, X., 2019. In situ synthesis of Au nanoparticles on viscose cellulose sponges for antibacterial activities. *Polymers* 11, 1281. <https://doi.org/10.3390/polym11081281>.
- Shankar, S., Oun, A.A., Rhim, J.-W., 2018. Preparation of antimicrobial hybrid nano-materials using regenerated cellulose and metallic nanoparticles. *Int. J. Biol. Macromol.* 107, 17–27. <https://doi.org/10.1016/j.ijbiomac.2017.08.129>.
- Subirats, J., Murray, R., Scott, A., Lau, C.H.-F., Topp, E., 2020. Composting of chicken litter from commercial broiler farms reduces the abundance of viable enteric bacteria, Firmicutes, and selected antibiotic resistance genes. *Sci. Total Environ.* 746, <https://doi.org/10.1016/j.scitotenv.2020.141113> 141113.
- Tsai, T.-T., Huang, T.-H., Chang, C.-J., Yi-Ju Ho, N., Tseng, Y.-T., Chen, C.-F., 2017. Antibacterial cellulose paper made with silver-coated gold nanoparticles. *Sci. Rep.* 7, 3155. <https://doi.org/10.1038/s41598-017-03357-w>.
- Velmurugan, P., Shim, J., Bang, K.-S., Oh, B.-T., 2016. Gold nanoparticles mediated coloring of fabrics and leather for antibacterial activity. *J. Photochem. Photobiol., B* 160, 102–109. <https://doi.org/10.1016/j.jphotobiol.2016.03.051>.
- Venkateswara Rao, A., Ashok, B., Uma Mahesh, M., Venkata Subbareddy, G., Chandra Sekhar, V., Venkata Ramanamurthy, G., Varada Rajulu, A., 2019. Antibacterial cotton fabrics with *in situ* generated silver and copper bimetallic nanoparticles using red sanders powder extract as reducing agent. *Int. J. Polym. Anal. Charact.* 24, 346–354. <https://doi.org/10.1080/1023666X.2019.1598631>.
- Wang, R., Zhang, M., Ge, B., Zhang, L., Zhou, J., Liu, S., Jiao, T., 2020. Facile preparation of black phosphorus-based rGO-BP-Pd composite hydrogels with enhanced catalytic reduction of 4-nitrophenol performances for wastewater treatment. *J. Mol. Liq.* 310, <https://doi.org/10.1016/j.molliq.2020.113083> 113083.
- Xiao, X., Zhao, W., Liang, J., Sauer, K., Libera, M., 2020. Self-defensive antimicrobial biomaterial surfaces. *Colloids Surf., B* 192, <https://doi.org/10.1016/j.colsurfb.2020.110989> 110989.
- Yousefi, H., Faezipour, M., Hedjazi, S., Mousavi, M.M., Azusa, Y., Heidari, A.H., 2013. Comparative study of paper and nanopaper properties prepared from bacterial cellulose nanofibers and fibers/-ground cellulose nanofibers of canola straw. *Ind. Crops Prod.* 43, 732–737. <https://doi.org/10.1016/j.indcrop.2012.08.030>.
- Zhang, C., Zhou, M., Liu, S., Wang, B., Mao, Z., Xu, H., Zhong, Y., Zhang, L., Xu, B., Sui, X., 2018. Copper-loaded nanocellulose sponge as a sustainable catalyst for regioselective hydroboration of alkynes. *Carbohydr. Polym.* 191, 17–24. <https://doi.org/10.1016/j.carbpol.2018.03.002>.
- Zheng, G., Polavarapu, L., Liz-Marzán, L.M., Pastoriza-Santos, I., Pérez-Juste, J., 2015. Gold nanoparticle-loaded filter paper: a recyclable dip-catalyst for real-time reaction monitoring by surface enhanced Raman scattering. *Chem. Commun.* 51, 4572–4575. <https://doi.org/10.1039/C4CC09466B>.